Critical Role of Side-Chain Attachment Density on the Order and Device Performance of Polythiophenes

R. Joseph Kline,[†] Dean M. DeLongchamp,*[,†] Daniel A. Fischer,[†] Eric K. Lin,[†] Lee J. Richter,[†] Michael L. Chabinyc,[‡] Michael F. Toney,[§] Martin Heeney,[||,#] and Iain McCulloch[⊥]

National Institute of Standards and Technology, Gaithersburg, Maryland 20899; Palo Alto Research Center, Palo Alto, California 94304; Stanford Synchrotron Radiation Laboratory, Menlo Park, California 94025; Merck Chemicals, Southampton, UK S016 7QD; and Department of Chemistry, Imperial College of London, London, UK SW7 2AZ

Received April 17, 2007; Revised Manuscript Received August 2, 2007

ABSTRACT: High performance, solution processable semiconductors are critical to the realization of low cost, large area electronics. We show that a signature molecular packing motif—side-chain interdigitation—correlates to high performance for a large and important class of organic semiconductors. The side chains of recently developed high performance copolymers of poly(alkylthiophenes) can and do interdigitate substantially, whereas they do not in the most common form of the extensively studied, lower performance poly(alkythiophenes). Side-chain interdigitation provides a mechanism for three-dimensional ordering; without it, poly(alkylthiophenes) are limited to small domains and poor performance. We propose the synthetic design rule that three-dimensional ordering is promoted by side-chain attachment densities sufficiently low to permit interdigitation.

Semiconducting polymers are promising candidate active layers in low cost/large area electronic applications such as organic-light-emitting diodes,[1,2] photovoltaic cells,[3,4] and thin-film transistors (TFT).[5,6] Adding side chains to semiconducting molecules renders them solution processable, enabling printed electronics on flexible substrates. Side chains also strongly influence the macromolecular order necessary to achieve high performance: bulky groups inhibit ordering,[7] small chiral groups cause backbone helicity,[8] and linear alkanes promote order.[9] Additionally, regioregularity,[9,10] casting solvent,[11,12] casting conditions,[13] substrate surface chemistry,[14,15] and relative molecular mass (MW)[16,17] have been shown to influence the polymer morphology and charge transport.

Regioregular poly(3-hexylthiophene) (P3HT), currently the most extensively studied solution processable semiconductor for TFT applications, forms a lamellar structure of π-orbital stacked conjugated backbones separated by regions of alkyl side chains.[9] Under optimal conditions, these domains orient nominally edge-on with the π-stacking in the plane of the substrate, giving rise to two-dimensional charge transport.[10] More recently, poly[5,5′-bis(3-dodecyl-2-thienyl)-2,2′-bithiophene)] (PQT)[18] and poly-(2,5-bis(3-alkylthiophene-2-yl)thieno[3,2-b]thiophenes) (pBTTTs)[19] have exhibited more ordered film structures and higher charge carrier mobilities than P3HT. Figure 1 compares atomic force microscopy (AFM) images of P3HT and pBTTT-C_{12} films characterized in this study. The P3HT film has a nodular structure with ≈10 nm domains while the pBTTT-C_{12} film has well-defined molecular terraces extending laterally for up to several microns. The terrace step height corresponds to the lamellar spacing measured in X-ray diffraction (XRD) (vide infra), indicating that the image is a true visualization of the lamellar packing motif previously inferred from XRD (Figure 1C).

In this report, we show that the attachment density of side chains, through its effect on side-chain interdigitation, correlates to the maximum extent of three-dimensional order and device performance attainable for a film of a semiconducting polymer with regularly spaced side chains. Since the side-chain attachment density is determined by the chemical structure of the monomer, it is an intrinsic property of the polymer independent of processing history, MW, or side-chain length. The influence of side-chain attachment density explains the success of the most recent generation of alkyl-substituted polythiophenes. The side-chain attachment densities of both pBTTT and PQT are sufficiently low to permit the interdigitation of side chains belonging to vertically adjacent layers, promoting three-dimensional order. The side-chain density of P3HT, on the other hand, is too large to allow interdigitation. Contrary to a common conceptual model depicting crystals with interdigitated side chains, P3HT instead has a two-dimensionally ordered, smectic-like structure without registry between layers.

Methods

pBTTT-C_{10}, -C_{12}, and -C_{14} were synthesized as previously reported with number-average relative molecular masses (M_n) of 27 000, 28 000, and 28 000 g/mol and polydispersities of 2.3, 1.8, and 2.0, respectively, as determined by GPC against polystyrene standards.[19] The preparations of pBTTT-C_{16} and -C_{18} are reported in the Supporting Information. The pBTTT films were cast from a 5 mg/mL solution in 1,2-dichlorobenzene at 1500(2π) rad/min with an acceleration of 100(2π) rad/min/s onto substrates treated with octyltrichlorosilane (OTS) and subsequently heated to 180 °C on a hot plate for 5 min.[20] PQT with a MW of 23 000 g/mol and polydispersity of 1.3 was obtained as a ≈0.3% dispersion in 1,2-dichlorobenzene from Xerox Research Centre of Canada.[18] Films were formed by spin-casting on OTS treated substrates by spinning at 1000(2π) rad/min and heated to 130 °C on a hot plate for 15−20 min. Poly(3-hexylthiophene) (P3HT) was obtained from Plextronics, Inc., with a M_n of 18 000 g/mol. P3HT films were cast

* Corresponding author. E-mail: dean.delongchamp@nist.gov.
[†] National Institute of Standards and Technology.
[‡] Palo Alto Research Center.
[§] Stanford Synchrotron Radiation Laboratory.
[||] Merck Chemicals.
[⊥] Imperial College of London.
[#] Present address: Department of Materials, Queen Mary, University of London, London UK E1 4NS.

10.1021/ma0709001 CCC: $37.00
Published on Web 10/04/2007

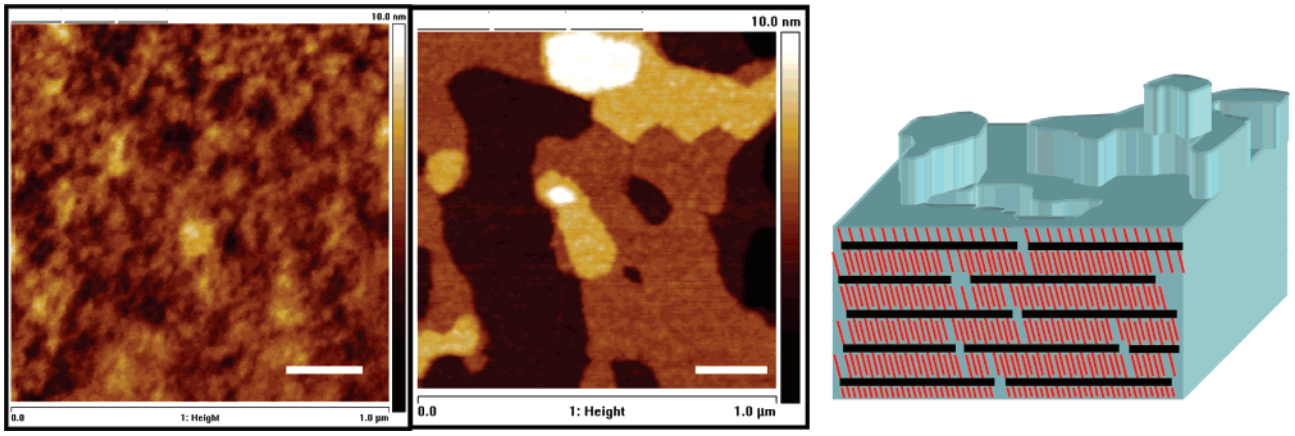

Figure 1. AFM height images of films of (a) P3HT and (b) pBTTT-C_{12} after heating to 180 °C for 5 min. Scale bar corresponds to 200 nm. (c) Schematic diagram showing the edge-on arrangement of molecules in the terraces. The black and red lines correspond to the conjugated backbone and side chains, respectively.

from a 5 mg/mL solution in chloroform at 1500(2π) rad/min onto substrates treated with OTS and heated to 180 °C on a hot plate for 5 min. All films were nominally 20−30 nm thick.

AFM was performed in tapping mode on either a multimode or dimension microscope (Veeco) with silicon cantilevers (Nanosensors).[21] Infrared (IR) spectroscopy was performed using a polarized Brewster's angle transmission geometry.[22] Near-edge X-ray absorption fine-structure (NEXAFS) was performed at NIST beamline U7A at the National Synchrotron Light Source. Grazing incidence X-ray scattering (GIXS) was performed on beamline 11-3, and specular diffraction was performed on beamline 2-1 at the Stanford Synchrotron Research Laboratory.[23]

Results and Discussion

I. Experimental Determination of Side-Chain Interdigitation. If an alkyl-substituted polythiophene thin film is sufficiently ordered and oriented, the extent of side-chain interdigitation can be determined from the lamellar spacing, side-chain length, and side-chain tilt away from the lamella normal.[20] Because no single measurement can determine the degree of interdigitation, we use a combination of XRD to measure lamellar spacing and polarized IR transmission spectroscopy and near-edge X-ray fine-structure spectroscopy (NEXAFS) to measure side-chain tilt. NEXAFS determines the orientation of the alkane chain long axis, while polarized IR determines the tilt angles of the mutually orthogonal transition dipole moments for the methylene symmetric and antisymmetric stretches. Polarized IR can also determine the level of local structural order of the alkane chain through the frequency of the methylene antisymmetric stretch. Values near 2918 cm^{-1} indicate highly ordered and all-trans alkane chains, while those near 2928 cm^{-1} indicate liquidlike alkane chains.[24] The methylene antisymmetric stretch locations (see Supporting Information) for P3HT, PQT, and pBTTT-C_{12} were 2925.9, 2921.9, and 2920.0 cm^{-1}, respectively (all $\pm$0.2 cm^{-1}). Therefore, the hexyl chains of P3HT are liquidlike and highly disordered,[22] whereas the dodecyl chains of pBTTT-C_{12} are nearly all-trans.[20] The effect of side-chain length will be discussed in more detail later in this paper.

Both NEXAFS and polarized IR measure the orientation distribution average of $\cos^2(\theta)$, where θ is the tilt of the side-chain director relative to substrate normal. The orientation of our films is such that the normal of the unit cell basal plane (a^*) is parallel to the substrate normal (as shown by specular XRD and AFM). We assume that the distribution of tilts is narrow and report θ as the side-chain tilt angle with respect to the normal of the unit cell basal plane (a^*).[20] The side-chain

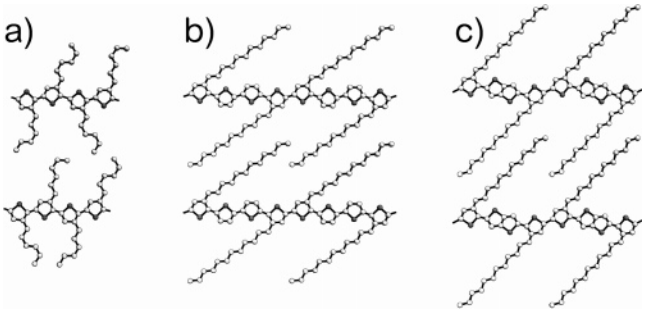

Figure 2. Illustration of side-chain structure for (a) P3HT, (b) PQT, and (c) pBTTT-C_{12}. The measured side-chain tilts are relative to the normal of the basal plane (horizontal plane in this figure). The azimuth of the tilt was arbitrarily fixed parallel to the backbone, and the noninterdigitated regions of PQT and pBTTT were drawn as all-trans for visual clarity. The real structure likely involves rotation of the side chains out of the plane of the backbone. Additionally, the noninterdigitated region is likely to be disordered and is discussed in detail in section III.

tilt angles for P3HT, PQT, and pBTTT-C_{12} are then 56°, 55°, and 44°, respectively. For both P3HT and PQT, the observed angle is near the "magic angle" of 54.7° and is equally consistent with a random distribution of tilts or a single tilt at the given angle.[25] Because of the liquidlike conformation of the P3HT side chains and the distribution of domain orientations (vide infra), we interpret the result as a nearly isotropic distribution. For PQT, we interpret the result as a single tilt angle due to its well-ordered side chains and oriented lamella. Figure 2 shows the degree of interdigitation of PQT and pBTTT-C_{12} determined from the XRD lamellar spacing, the side-chain length, and the measured tilt. P3HT is shown with its liquidlike side chains. We note that for P3HT the assumption of all-trans side chains at the measured tilt results in an unphysical gap of $\approx$4.5 Å between lamellae, strongly supporting the conclusion of disordered side chains.

II. Side-Chain Packing Model. A simple close-packing model can clarify why the side chains of P3HT are not interdigitated, whereas the side chains of PQT and pBTTT-C_{12} are both moderately tilted and interdigitated. It is known from studies of self-assembled monolayers of alkanethiols[26] that the average chain tilt of tethered alkanes can be related to the areal attachment density. If the areal density of upright alkane chains is less than that of a dense aliphatic solid such as crystalline polyethylene (PE) (5.4×10^{14} cm^{-2}), van der Waals interactions will cause them to either tilt until repulsive interactions establish

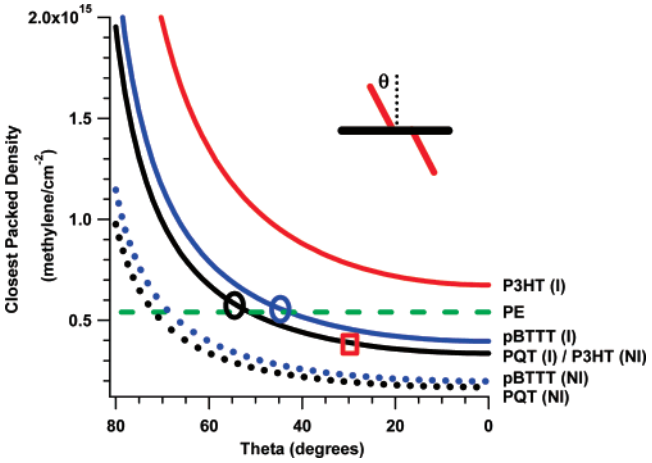

Figure 3. Variation in side-chain packing density with side chain tilt for P3HT, PQT, and pBTTT-C_{12}. The packing density of PE is shown for comparison. Circles denote experimentally measured tilts for PQT and pBTTT, while the square denotes the calculated, effective tilt for P3HT. (I and NI are interdigitated and noninterdigitated, respectively.)

a close-packed local density or to collapse into a disordered brush.

Vector analysis was used to calculate the local density of the closest-packed plane for P3HT, PQT, and pBTTT-C_{12} for a range of side-chain tilts with and without interdigitation (Figure 3). For each polymer, the areal attachment density is uniquely determined by the chemical structure of the polymer backbone and the experimentally measured π-stacking distance between adjacent backbones. The attachment density and the calculated local packing density are independent of side-chain length and the MW of the polymer (assuming a constant π-stacking distance). Since the π-stacking distance of well-packed conjugated polymers is similar ($\approx$3.8 Å), only the spacing of side chains along the backbone is synthetically controllable.

Within this packing density model, P3HT side chains cannot interdigitate because the predicted density of interdigitated chains is substantially higher than PE at all tilts. Even if the P3HT side chains were perfectly vertical, they would require an unphysical density almost 50% greater than PE to interdigitate, requiring compaction far beyond the van der Waals radii of the component methylenes. We note in Figure 3 the calculated P3HT tilt angle (red square) consistent with nominally straight, noninterdigitated hexyl chains for the measured lamellar spacing (16.7 Å). The methylene density for chains of this tilt is 72% of PE and comparable to that for liquid hexane (as expected for the degree of disorder measured by IR).

The significantly lower side-chain attachment density of PQT and pBTTT permit interdigitation at moderate tilts. In fact, there is a striking correlation between the experimentally determined side-chain tilts of PQT and pBTTT-C_{12} and the tilts required to approach PE density as determined by this packing density model. The experimentally determined side-chain tilts are shown in Figure 3 (circles) and closely correspond to the intersection with PE packing density. We note that it is possible for the side chains of PQT and pBTTT-C_{12} to achieve PE density without interdigitation, but such packing would require more extreme side chain tilts of 72° and 69°, respectively. Clearly, the interdigitated structure is the favored room temperature state for both PQT and pBTTT.

III. Effect of Tilting on Side-Chain Packing. The extent of interdigitation can be determined by comparing the lamellar spacing calculated from the side-chain tilt to the measured lamellar spacing. The measured lamellar spacing of both PQT and pBTTT-C_{12} is larger than what would be expected for full interdigitation, indicating partial interdigitation (Figure 2). The interdigitated regions and the backbone are separated by a presumably underdense, noninterdigitated region. We hypothesize that this noninterdigitated region compensates for the mismatch between the tilt of the interdigitated region and the angle enforced by covalent attachment to the sp^2 hybridized β position of thiophene. Accommodating this mismatch presumably limits further penetration of the opposite interdigitating side chain and determines the allowed extent of interdigitation. This hypothesis suggests that the noninterdigitated region should have a fixed size independent of side-chain length.

This hypothesis is consistent with IR results for the degree of side-chain order in a series of pBTTTs with varying side chain length. The lower density of the methylenes in the noninterdigitated region, along with possible bond angle distortions to accommodate the conflicting packing requirements of the chains and backbone, likely results in less order than in the interdigitated region. Therefore, if the noninterdigitated region has a fixed size, the average concentration of gauche defects should decrease as side-chain length increases. This hypothesis is supported in Figure 4a, which shows that the methylene

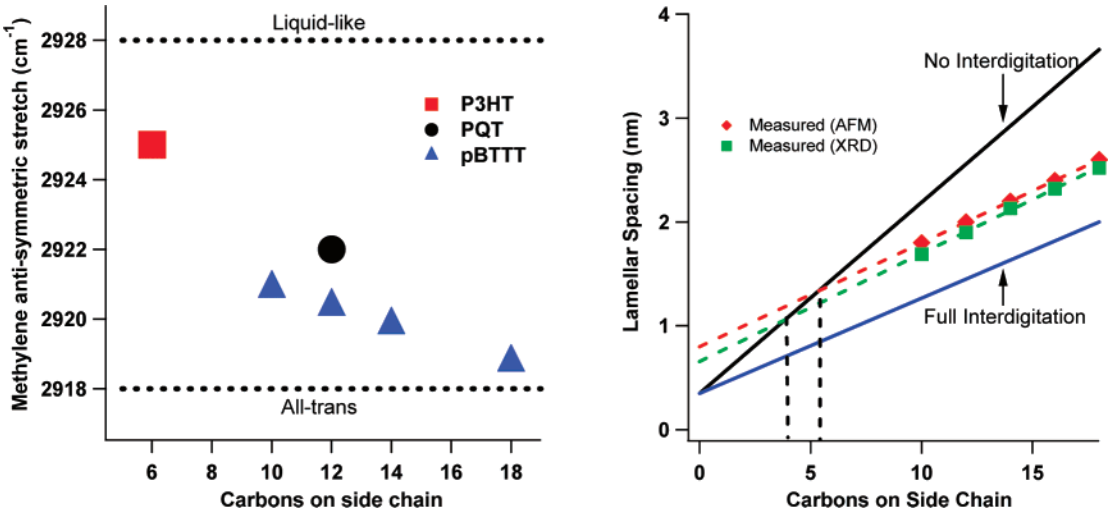

Figure 4. (a) Position of the methylene antisymmetric stretch and (b) lamellar spacing of pBTTT as measured by XRD and AFM as a function of side-chain length. The solid lines in (b) are the calculated spacings for a 45° side-chain tilt for the case of full interdigitation and no interdigitation while the dashed lines are the linear fit of the data points. The vertical dashed lines mark the intersection of the linear fits with the calculated spacing for no interdigitation. The standard uncertainty of AFM step height and XRD *d*-spacing are 5% and 1%, respectively.

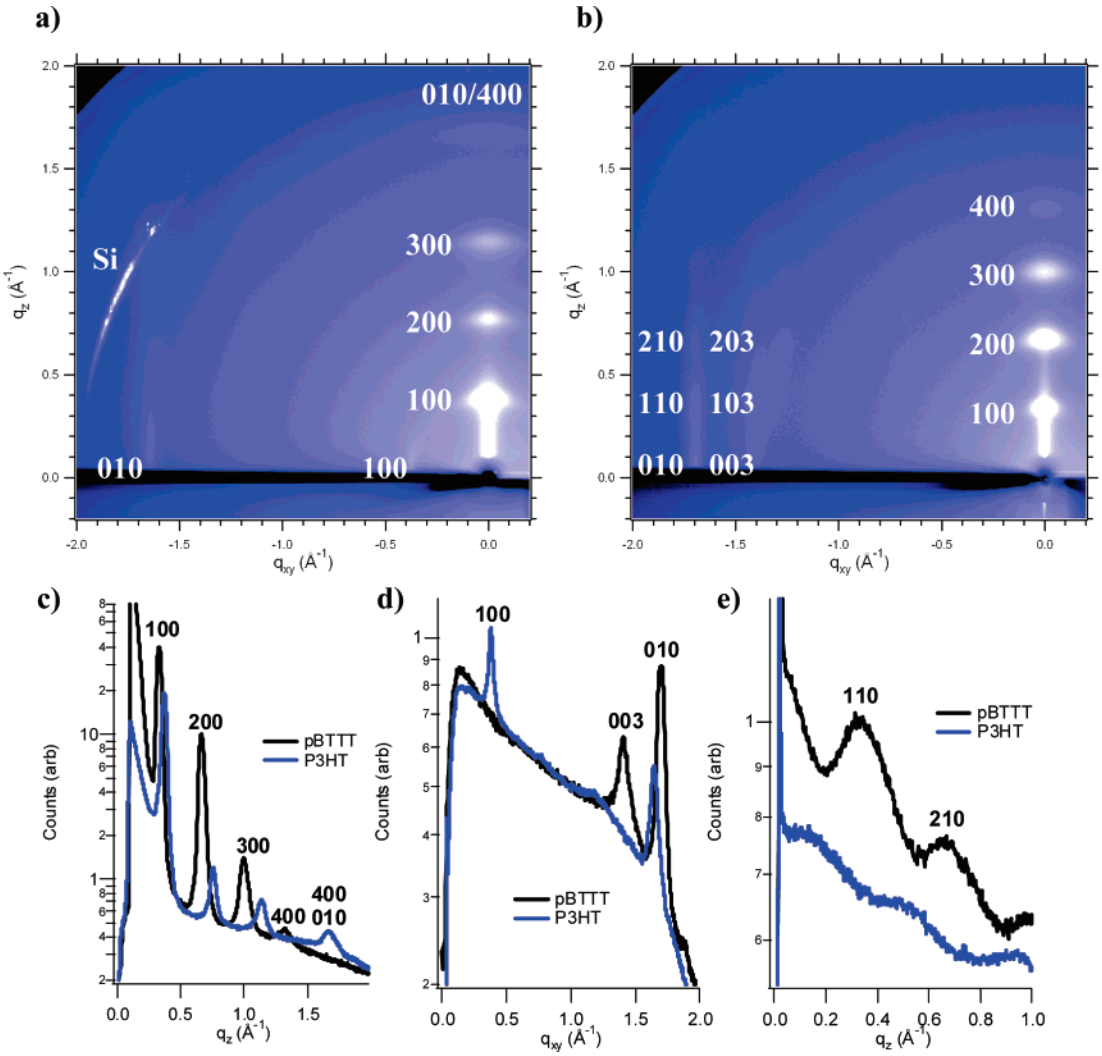

Figure 5. Two-dimensional GIXD comparing (a) P3HT to (b) pBTTT-C_{12} thin films. (c) and (d) show q_z and q_{xy} scans through the origin, respectively, while (e) shows a vertical scan through the *h*10 peak series. The standard uncertainty of q is 5%.

antisymmetric stretch position systematically decreases from 2921 to 2919 cm^{-1} as the number of carbons in the pBTTT side chains increases from 10 to 18. Figure 4a also shows that both P3HT and PQT do not fall on the line that fits the pBTTT values. For PQT, this discrepancy is likely due to the fact that the larger tilt of the interdigitated regions (as compared to those of pBTTT) requires a larger noninterdigitated region to reconcile the tilt mismatch. This result is in agreement with the experimentally determined packing structure for PQT shown in Figure 2.

The fixed size of the noninterdigitated region can also be confirmed by comparing the lamellar spacing of pBTTTs with varying side-chain length. Shown in Figure 4b are the lamellar spacings determined by specular XRD and estimated from AFM terrace heights. The lamellar spacings determined by XRD are slightly less than those determined by AFM, although the difference is comparable to the calibration accuracy of the AFM. The lamellar spacing exhibits a pronounced linear relationship with side-chain length with a *y*-intercept of 0.66 ± 0.05 and 0.8 ± 0.1 nm for XRD and AFM, respectively. For fully interdigitated chains with a common tilt angle, one would expect a linear relationship with a *y*-intercept equal to the excluded volume of the conjugated backbone (≈0.4 nm). The observation of a larger intercept is consistent with partially interdigitated side chains with a noninterdigitated region composed of about 4−5 methylene units. If the size of the noninterdigitated region is independent of chain length, the slope of the fit to lamellar spacing vs chain length is determined by the side-chain tilt angle within the interdigitated region. The value calculated for the lamellar spacing measured by AFM and XRD correspond to a tilt of 40 ± 3° and 37 ± 2°, respectively, slightly less than that measured by IR and NEXAFS.

A similar linear relationship between lamellar spacing and side-chain length has been previously reported for P3ATs,[27,28] corresponding to a side-chain tilt angle of the densely packed region of ≈50°, in agreement with the value predicted by the packing model for noninterdigitated P3ATs. Noninterdigitated structures, such as the P3ATs, will have a less dense region near the side-chain attachment to the backbone similar to the noninterdigitated region of partially interdigitated structures to accommodate the tilt mismatch.

IV. P3HT and Interdigitation. In general, there appears to be some confusion regarding the potential for P3HT side-chain interdigitation in the recent literature. Schematics showing interdigitation[29−31] and discussions about interdigitation effects on morphology[32] appear commonplace even though there are no direct reports providing evidence of interdigitation. Epitaxial monolayers of P3ATs on graphite[33] imaged by scanning tunneling microscopy have been described as "interdigitated"; however, their two-dimensional packing is dominated by the lattice mismatch and face-on interaction with the underlying graphite substrate and is quite

different from the upright, three-dimensional packing present in thin films.

Our conclusion that the side chains of P3HT do not interdigitate agrees with early diffraction studies of P3ATs. The most commonly reported polymorph, type I, was predicted in all early structure studies to be noninterdigitated with tilted side chains[27,28,34,35] while the metastable type II form was most consistent with vertically oriented side chains that were interdigitated. The chains of the type II form are able to interdigitate because of an increase in the π-stacking distance of 24% to 4.7 Å.[34] This lattice expansion decreases the areal attachment density precisely enough to allow vertically oriented, interdigitated side chains to achieve the packing density of PE, as predicted by our packing model. The increased π-stacking distance also substantially reduces the electronic overlap between neighboring molecules, severely hindering charge transport for type II P3ATs.[34] Clearly, interdigitation at the expense of efficient π-stacking will not improve charge transport. The type II polymorph is rarely reported. It is usually only obtained as a minority component of a type I film formed by slow solvent casting, and it readily converts to type I upon heating. Its metastable nature is explained by a competition between the energy reduction of backbone π-stacking with that of side-chain interdigitation. Because the π-stacking interaction provides a greater energetic reduction,[20] smaller π-stacking distances are favored and noninterdigitated forms of P3ATs are the thermodynamically favored state.

V. Implications of Interdigitation. Without side-chain interdigitation, there exists no strong mechanism to preserve registry between adjacent P3HT lamellae. The disordered side chains of P3HT further reduce the possibility of layer registry, leading to an inability of P3HT to exhibit order greater than smectic-like layers. We speculate that this lack of interlayer registry is likely the origin of the typical small P3HT domain size and its limited charge transport.

In contrast, polymers such as PQT and pBTTT with substantial interdigitation do possess a mechanism for interlayer registry. This three-dimensional registry should enhance lateral ordering because the closely packed, interdigitated side chains help to preserve the structure by interlocking adjacent layers. This advantage explains the greatly increased domain size (from $\approx$10 nm to micrometers) and improved charge transport (from 0.1 to 0.5 $cm^2/(V\ s)$) in these polymer semiconductors.

Different extents of three-dimensional ordering are confirmed by GIXD shown in Figure 5. The patterns of pBTTT contain higher order mixed index peaks of the *h*10 and *h*03 series, confirming three-dimensional ordering.[23] The PQT pattern also has these same mixed index peaks.[36] The pattern of P3HT, on the other hand, consists primarily of peaks in the *h*00 and 0*k*0 series, as expected from diffraction of a low-order smectic phase and consistent with previous reports of P3HT GIXD.[10,37] The presence of *h*00 peaks in-plane shows that the film is also a combination of highly oriented, edge-on domains and misoriented plane-on domains. The sharp Bragg diffraction rocking curves previously reported for highly oriented P3HT films[15] have also been reported for other smectic thin films.[38,39] This high level of orientation is caused by the layers conforming to a flat substrate and does not require crystallinity or three-dimensional ordering. Weak three-dimensional ordering has been reported for P3ATs with dodecyl chains.[27,34] This ordering is likely directed by the corrugation of adjacent ordered arrays of terminal methyl groups formed by the longer side chains and does not occur in P3HT because the chains are too disordered. This weak three-dimensional ordering apparently does not improve the charge transport in P3DDT because its reported charge carrier mobility is several orders of magnitude worse than P3HT.[40]

In summary, we have demonstrated that the attachment density of alkane side chains on thiophene-based polymers controls side-chain interdigitation between lamellae. The lack of interdigitation in P3HT leads to a lack of registry between lamellae, resulting in the poor order typically observed by XRD and AFM. PQT and pBTTT, on the other hand, have three-dimensional order and larger domains. This interdigitation model explains why PQT and pBTTT have superior charge transport and provides clear synthetic design rules for this important class of high performance polymer semiconductors.

Acknowledgment. R.J.K. thanks support from the NIST-NRC program. Portions of this research were carried out at the Stanford Synchrotron Radiation Laboratory, a national user facility operated by Stanford University on behalf of the U.S. Department of Energy, Office of Basic Energy Sciences.

Supporting Information Available: Detailed description of side-chain density calculation, synthesis of pBTTT-C_{16} and -C_{18}, XRD measurements, and measurements of PQT tilt. This material is available free of charge via the Internet at http://pubs.acs.org.

References and Notes

(1) Heeger, A. *J. Phys. Chem. B* **2001**, *105*, 8475−8491.
(2) Friend, R.; Gymer, R.; Holmes, A.; Burroughes, J.; Marks, R.; Taliani, C.; Bradley, D.; Dos Santos, D.; Bredas, J.; Logdlund, M.; Salaneck, W. *Nature (London)* **1999**, *397*, 121−128.
(3) Coakley, K. M.; McGehee, M. D. *Chem. Mater.* **2004**, *16*, 4533−4542.
(4) Hoppe, H.; Sariciftci, N. S. *J. Mater. Res.* **2004**, *19*, 1924−1944.
(5) Chabinyc, M. L.; Salleo, A. *Chem. Mater.* **2004**, *16*, 4509−4521.
(6) Horowitz, G. *J. Mater. Res.* **2004**, *19*, 1946−1962.
(7) Bao, Z.; Lovinger, A. *Chem. Mater.* **1999**, *11*, 2607−2612.
(8) Langeveld-Voss, B. M. W.; Janssen, R. A. J.; Meijer, E. W. *J. Mol. Struct.* **2000**, *521*, 285−301.
(9) Bao, Z.; Dodabalapur, A.; Lovinger, A. *Appl. Phys. Lett.* **1996**, *69*, 4108−4110.
(10) Sirringhaus, H.; Brown, P. J.; Friend, R. H.; Nielsen, M. M.; Bechgaard, K.; Langeveld-Voss, B. M. W.; Spiering, A. J. H.; Janssen, R. A. J.; Meijer, E. W.; Herwig, P.; de Leeuw, D. M. *Nature (London)* **1999**, *401*, 685−688.
(11) Chang, J. F.; Sun, B. Q.; Breiby, D. W.; Nielsen, M. M.; Solling, T. I.; Giles, M.; McCulloch, I.; Sirringhaus, H. *Chem. Mater.* **2004**, *16*, 4772−4776.
(12) Kline, R. J.; McGehee, M. D.; Kadnikova, E. N.; Liu, J.; Frechet, J. M. J.; Toney, M. F. *Macromolecules* **2005**, *38*, 3312−3319.
(13) DeLongchamp, D. M.; Vogel, B. M.; Jung, Y.; Gurau, M. C.; Richter, C. A.; Kirillov, O. A.; Obrzut, J.; Fischer, D. A.; Sambasivan, S.; Richter, L. J.; Lin, E. K. *Chem. Mater.* **2005**, *17*, 5610.
(14) Salleo, A.; Chabinyc, M.; Yang, M.; Street, R. *Appl. Phys. Lett.* **2002**, *81*, 4383−4385.
(15) Kline, R. J.; McGehee, M. D.; Toney, M. F. *Nat. Mater.* **2006**, *5*, 222−228.
(16) Kline, R. J.; McGehee, M. D.; Kadnikova, E. N.; Liu, J.; Frechet, J. M. J. *Adv. Mater.* **2003**, *15*, 1519−1522.
(17) Zen, A.; Pflaum, J.; Hirschmann, S.; Zhuang, W.; Jaiser, F.; Asawapirom, U.; Rabe, J. P.; Scherf, U.; Neher, D. *Adv. Funct. Mater.* **2004**, *14*.
(18) Ong, B. S.; Wu, Y. L.; Liu, P.; Gardner, S. *J. Am. Chem. Soc.* **2004**, *126*, 3378−3379.
(19) McCulloch, I.; Heeney, M.; Bailey, C.; Genevicius, K.; MacDonald, I.; Shkunov, M.; Sparrowe, D.; Tierney, S.; Wagner, R.; Zhang, W.; Chabinyc, M. L.; Kline, R. J.; McGehee, M. D.; Toney, M. F. *Nat. Mater.* **2006**, *5*, 328−333.
(20) DeLongchamp, D. M.; Kline, R. J.; Lin, E. K.; Fischer, D. A.; Richter, L. J.; Lucas, L. A.; Heeney, M.; McCulloch, I.; Northrup, J. E. *Adv. Mater.* **2007**, *19*, 833−837.
(21) Certain equipment, instruments or materials are identified in this paper in order to adequately specify the experimental details. Such identification does not imply recommendation by the National Institute of Standards and Technology nor does it imply the materials are necessarily the best available for the purpose.
(22) Gurau, M. C.; DeLongchamp, D. M.; Vogel, B. M.; Lin, E. K.; Fischer, D. A.; Sambasivan, S.; Richter, L. J. *Langmuir* **2007**, *23*, 834−842.

(23) Chabinyc, M. L.; Toney, M. F.; Kline, R. J.; McCulloch, I.; Heeney, M. *J. Am. Chem. Soc.* **2007**, *129*, 3226−3237.
(24) MacPhail, R. A.; Strauss, H. L.; Snyder, R. G.; Elliger, C. A. *J. Phys. Chem.* **1984**, *88*, 334−341.
(25) Stöhr, J. *NEXAFS Spectroscopy*; Springer-Verlag: Berlin, 1992.
(26) Love, J. C.; Estroff, L. A.; Kriebel, J. K.; Nuzzo, R. G.; Whitesides, G. M. *Chem. Rev.* **2005**, *105*, 1103−1170.
(27) Tashiro, K.; Kobayashi, M.; Kawai, T.; Yoshino, K. *Polymer* **1997**, *38*, 2867−2879.
(28) Yamamoto, T.; Komarudin, D.; Arai, M.; Lee, B. L.; Suganuma, H.; Asakawa, N.; Inoue, Y.; Kubota, K.; Sasaki, S.; Fukuda, T.; Matsuda, H. *J. Am. Chem. Soc.* **1998**, *120*, 2047−2058.
(29) McCullough, R. D. *Adv. Mater.* **1998**, *10*, 93−116.
(30) Sirringhaus, H.; Tessler, N.; Friend, R. H. *Science* **1998**, *280*, 1741−1744.
(31) Kim, D. H.; Park, Y. D.; Jang, Y.; Yang, H.; Kim, Y. H.; Han, J. I.; Moon, D. G.; Park, S.; Chang, T.; Chang, C.; Joo, M.; Ryu, C. Y.; Cho, K. *Adv. Mater.* **2005**, *15*, 77−82.
(32) Malik, S.; Nandi, A. K. *J. Polym. Sci., Part B: Polym. Phys.* **2002**, *40*, 2073−2085.
(33) Mena-Osteritz, E.; Meyer, A.; Langeveld-Voss, B. M. W.; Janssen, R. A. J.; Meijer, E. W.; Bauerle, P. *Angew. Chem.., Int. Ed.* **2000**, *39*, 2680.
(34) Prosa, T. J.; Winokur, M. J.; McCullough, R. D. *Macromolecules* **1996**, *29*, 3654−3656.
(35) Meille, S.; Romita, V.; Caronna, T.; Lovinger, A.; Catellani, M.; Belobrzeckaja, L. *Macromolecules* **1997**, *30*, 7898−7905.
(36) Chabinyc, M. L.; Jimison, L.; Salleo, A.; Toney, M. F. Manuscript in preparation.
(37) Yang, H.; Shin, T. J.; Yang, L.; Cho, K.; Ryu, C. Y.; Bao, Z. *Adv. Funct. Mater.* **2005**, *15*, 671−676.
(38) Geer, R. E.; Shashidhar, R. *Phys. Rev. E* **1995**, *51*, R8−R11.
(39) Geer, R. E.; Shashidhar, R.; Thibodeaux, A. F.; Duran, R. S. *Phys. Rev. Lett.* **1993**, *71*, 1391−1394.
(40) Babel, A.; Jenekhe, S. A. *Synth. Met.* **2005**, *148*, 169−173.

MA0709001